50 YEARS MRS

Hybrid materials approaches for bioelectronics

Hedan Bai, Ziying Hu, and John A. Rogers*

Bioelectronic systems are emerging technologies with unique capabilities for establishing bidirectional biophysical and biochemical interfaces to soft living tissues. Applications range from tools for biomedical research on organoids and animal models to sensing and therapeutic platforms for addressing patient needs. Recent advances in materials science, materials processing techniques, and assembly/integration methods establish the foundations for progress in this area, with a growing collection of successful examples of translation into commercial products. This article summarizes our own work in this area, with an emphasis on hybrid approaches that combine both organic and inorganic materials into engineered composite structures optimized to support functional requirements, including physical/chemical levels of biocompatibility, high-performance electronic/microfluidic operation, tissue-like mechanical properties and geometries, and in some cases, fully bioresorbable designs and/or three-dimensional (3D) layouts. System-level examples that leverage these ideas span (1) epidermal platforms that probe the electrical, thermal, mechanical, and chemical properties of the skin and underlying physiological processes for diagnostic purposes; (2) implantable devices that combine sensors and therapeutic actuators under closed-loop feedback control through intimate interfaces to various tissues/organs; (3) bioresorbable electronic systems as temporary implants that support a desired operational time frame and then harmlessly degrade within the body; and (4) 3D mesoscale networks that integrate with tissue constructs across volumetric spaces for multimodal neuromodulation, sensing, and manipulation. We conclude with an overview of the current state of the field and a summary of research opportunities in hybrid materials approaches as the basis for continued advances in bioelectronics.

Introduction

Advanced electronics technologies that can intimately integrate with biological systems have the potential to accelerate progress in biomedical research and to improve strategies in patient care. Progress in materials science provides the foundations in these types of bioelectronic systems, uniquely defined by characteristics, ranging from soft mechanical properties to bioresorbable constituent chemistries, that are unavailable with conventional semiconductor devices.[1–4] Some of the most successful approaches combine collections of organic and inorganic materials in strategic layouts designed to satisfy the full scope of required properties, from electronic function to biocompatible physical and chemical characteristics. Although many research groups have reported impressive progress in this area, the following article focuses on our work toward this hybrid strategy, spanning polymeric electronic materials to semiconductor nanomaterials and methods for patterning and integrating them into functional systems. The content includes an overview of various methods that blend unconventional and conventional materials in unusual two- and three-dimensional (2D/3D) geometries guided by mechanics modeling, as a form of deterministic composite engineering. Examples with demonstrated utility include skin-like electronic/microfluidic platforms as sensors of physiological health, tissue-like implantable devices as tools for neuroscience research, bioresorbable wireless systems as "electronic medicines," and 3D mesoscale frameworks as functional interfaces to small-scale tissue structures. A concluding section summarizes the current state of the field and highlights opportunities for further research in hybrid materials approaches for bioelectronics.

Hedan Bai, Querrey Simpson Institute for Bioelectronics, Northwestern University, Evanston, USA; hedan.bai@mat.ethz.ch
Ziying Hu, Querrey Simpson Institute for Bioelectronics, Northwestern University, Evanston, USA; ziying.hu@northwestern.edu
John A. Rogers, Querrey Simpson Institute for Bioelectronics, Northwestern University, Evanston, USA; Department of Materials Science and Engineering, Mechanical Engineering, Biomedical Engineering, Chemistry, Electrical Engineering and Computer Science, Dermatology, Northwestern University, Evanston, USA; Department of Neurological Surgery and Dermatology, Feinberg School of Medicine, Northwestern University, Chicago, USA; jrogers@northwestern.edu
*Corresponding author
doi:10.1557/s43577-023-00620-6

Hybrid materials approach

The development of high-performance microsystems technologies in soft, biocompatible forms depends critically on advances in materials science—specifically in identifying materials and device architectures capable of establishing intimate, noninvasive interfaces with the 3D, curvilinear, dynamic, and heterogeneous living tissues, while supporting a broad range of functions in (opto-) electronics, microfluidics, and microelectromechanics. One approach relies on a complete set of organic electronic materials formed using the techniques of synthetic chemistry, as alternatives to the traditional complement of inorganics used in conventional technologies with planar, rigid formats.[4] A daunting challenge is in achieving adequate performance for practical applications and in creating a manufacturing infrastructure for scaled production. Alternatives based on emerging materials can also be considered, from carbon nanotubes to semiconductor nanowires and 2D materials.[1] Although these and other options do not suffer from severe performance limitations, all require further innovations in growth, patterning, and system integration for meaningful applications.

The hybrid approach summarized here combines unusual and conventional materials in a form of mechanics-guided composite engineering. Here, hard inorganics selected for their excellent electronic properties blend with soft elastomeric materials as supporting matrices and biointerfaces, to realize bioelectronic devices that meet the combined requirements of function, shape, and mechanics for integration with living organisms. Representative schemes involve inorganic electronic materials structured into ultrathin, micro-/nanoscale structures with "wavy" and/or "serpentine" shapes, often in open filamentary mesh geometries created using techniques that align with advanced capabilities in the semiconductor industry.[5] The methods of transfer printing allow for integration into elastomeric matrices and/or functional polymers, where covalent interfacial reactions bond these hard and soft components in lithographically defined patterns.

The resulting hard/soft composites exhibit a wide range of deterministic, precisely controllable mechanical properties that can be configured to match those of biological systems, while supporting a broad range of functions. **Table I** provides representative material examples commonly used in this hybrid approach, where inorganic materials with superior electrical properties—biocompatible chemistry and electrical conductivity (thin films of Au), semiconductor mobility (monocrystalline nanomembranes of Si), biofluid impermeability (thermally grown layers of SiO_2)—in engineered shapes yield effective elastic moduli and levels of stretchability that are comparable to those of soft tissues (modulus: $E \sim 1–10^2$ kPa, strain: $\varepsilon \sim 100\%$), orders of magnitudes softer than their intrinsic bulk properties ($E \sim 10^2$ GPa, $\varepsilon < 1\%$). Another feature of such types of hard/soft constructs is their ability to geometrically conform to irregular, textured, and curvilinear biological surfaces such as those of the skin and the brain.[6–8] This intimate device–tissue interface is essential for a range of diagnostic and therapeutic functions.

The general framework of this mechanics-guided hybrid approach supports sophisticated possibilities in tailoring the properties and geometries of the systems to match those of biological targets for integration. In one example, materials selections and layouts match not only the elastic properties of soft tissues, such as skin, in the linear regime of the stress–strain response curve, but also the full J-shape characteristics up to large values of strain, as well as diverse aspects of anisotropy and spatial heterogeneity.[9] For example, an open mesh electronic framework that consists of repeating triangular serpentine lattice, including filamentary Cr/Au electrodes (thickness: 7/100 nm) and a polyimide (PI, thickness: 2 μm) network embedded in a silicone elastomer (thickness: 60 μm) exhibits a stress–strain response dominated by buckling mechanics, and correspondingly low tangential modulus, at low strain, with strain-limiting characteristics and high tangential modulus, both characteristic of the mesh structure, at high strain. Mechanical modeling and inverse design strategies can yield soft, hybrid materials with deterministic stress–strain responses that can exactly match those measured directly from tissues of interest, across a wide range. **Figure 1**a shows experimentally measured J-shape curves of a PI network that resides in the middle of a silicone matrix, as designer composites, and their close correspondence to desired stress–strain responses of human skin, from different locations of the body.[9] Combinations of these and related mesh structures, with spatial variations, provide access to heterogeneous and anisotropic properties, such as gradients in stiffness and direction-dependent responses, as are common in biology.

Advanced forms of design leverage concepts in fractal mathematics, where self-similar geometries in the mesh structures can cover an arbitrary 2D space using well-established iterative rules and basic geometries. Patterns of high fractal order lead to sophisticated levels of structural flexibility, where the self-similarity corresponds, mechanically, to a hierarchy of springs. This scheme can be automated and paired with circuit design tools, to yield 2D spaces filled with traces of functional inorganic materials with similar layouts in fractal designs for dense electronic layouts, with spatial control over the elastic behavior to accommodate biaxial, radial, and anisotropic modes of deformation, with high stretchability (Figure 1b).[6] The sorts of strategies outlined in this section apply to broad classes of organic and inorganic materials, as illustrated specifically in the context of devices described in the following.

Epidermal electronics and microfluidics

These ideas in hybrid materials design enable a wide range of high-performance electronic devices and other microsystems technologies with biocompatible physical and chemical properties. A first reported system-level example is in skin-like, or "epidermal," electronics designed to establish intimate, conformal biointerfaces to the skin, with the ability

Table I. Representative materials and performance for the hybrid approach to bioelectronics.

Material	Mechanical Properties				Electrical Properties	
	Elastic Modulus		Elastic Stretchability		Conductivity	Water Vapor Permeability
	Intrinsic	Engineered Shapes	Intrinsic	Engineered Shapes		
Tissue						
Skin	5–10^4 kPa[9,49]	–	20–100%[9]	–	–	–
Heart muscle	20–200 kPa[50]		80–120%[51,52]			
Brain	1–2 kPa[53]		–			
Conductor						
Au	78 GPa	Serpentine	~0.3%	Serpentine 100%[6,54]	4×10^7 S m^{-1}	–
		120 kPa[8]		3D coil 150%[54,55]		
Semiconductor						
Si	130 GPa	Wavy nanomembrane	<1% (fracture)	Wavy 5.7%[56]	Mobility[57]	–
		160 kPa[45]		Ribbon 140%[57]	370 (n-), 130 (p-) $cm^2 V^{-1} s^{-1}$	
Dielectric/encapsulation						
Silicone elastomer	~1–10^4 kPa	–	~10–1000%	–	–	~100 $gm^{-2} d^{-1}$
Polyimide	2.5 GPa		~1%	Serpentine 100%[6,54]		–1 $gm^{-2} d^{-1}$
t-SiO_2	70 GPa		–	–		~10^{-7} $gm^{-2} d^{-1}$

to adapt to its complex contoured surfaces without mechanical, thermal, or mass-loading constraints even during large, time-variant deformations of the skin (Figure 1).[6,9] Beyond mechanical compliance, this intimate contact also minimizes electrical, mechanical, thermal, and optical impedances as the basis for high-precision measurements of the skin or of underlying physiological processes, for clinical-grade monitoring modalities. This generalized epidermal platform thus offers the ability to probe the electrical, thermal, mechanical, and chemical properties of the skin, and the function of tissues and organs, with high fidelity for diagnostic purposes; delivery of stimuli (e.g., electrical stimulation, mechanical vibration, thermal modulation) to the skin represents additional emerging opportunities in patient feedback. Two classes of possibilities can be considered: one reproduces measurements performed at hospitals, but without wires, with reduced costs and without constraints in measurement settings; the other supports translational functions that lie beyond the scope of existing medical technologies.

One example that demonstrates the hybrid materials approach in the former mode of use is in epidermal electronics for monitoring of premature babies in neonatal intensive care units (NICUs, **Figure 2**a). Approximately 300,000 newborn infants with great health risks pass into NICU facilities in the United States every year, where they receive complex diagnostic and therapeutic measures for survival and improvement of future quality of life. Continuous monitoring of the vital signs of these exceptional fragile, tiny infants currently requires multiple wired interfaces that create risks to skin injury, impede skin-to-skin infant–parental bonding, and frustrate even basic operations in clinical care. Epidermal electronic systems (EESs, Figure 2a) avoid these disadvantages, to provide a greatly preferred, untethered mode of monitoring of all vital signs (electrocardiograms [ECGs], photoplethysmograms [PPG], temperature) with a single pair of wireless, ultrathin, low-modulus devices that gently interface to the skin.[10] An EES consists of filamentary serpentine structures of metal (e.g., Au or Cu) traces that interconnect compact, thin integrated circuit components, all embedded in an encapsulating structure of poly(dimethylsiloxane) (PDMS) that defines a microfluidic chamber filled with a blended solution of a nontoxic ionic liquid (1-ethyl-3-methylimidazolium ethyl sulfate) and silica gel (pore size 6 nm) to mechanically decouple the interconnects and components from the PDMS and, thus, the underlying skin. Fractal geometries in conductive filamentary mesh constructs, as introduced previously, define electrodes for ECG with high coverage ratios while retaining stretchability. This collection of hybrid materials, in layouts guided by quantitative studies of their combined effective mechanical properties, provides overall effective stretchability ($\varepsilon \sim 16\%$) and elastic modulus ($E \sim 200$–300 kPa) that are comparable to the skin itself. The result minimizes interface stresses at the surface of the skin, yet allows robust adhesion with negligible risk for skin injury during removal, even with youngest neonates with the most fragile skin. Furthermore, the configuration of the electronic materials minimizes shadowing and radio-frequency interference during imaging with modern medical techniques used in the NICU, including magnetic resonance imaging and x-ray coherence

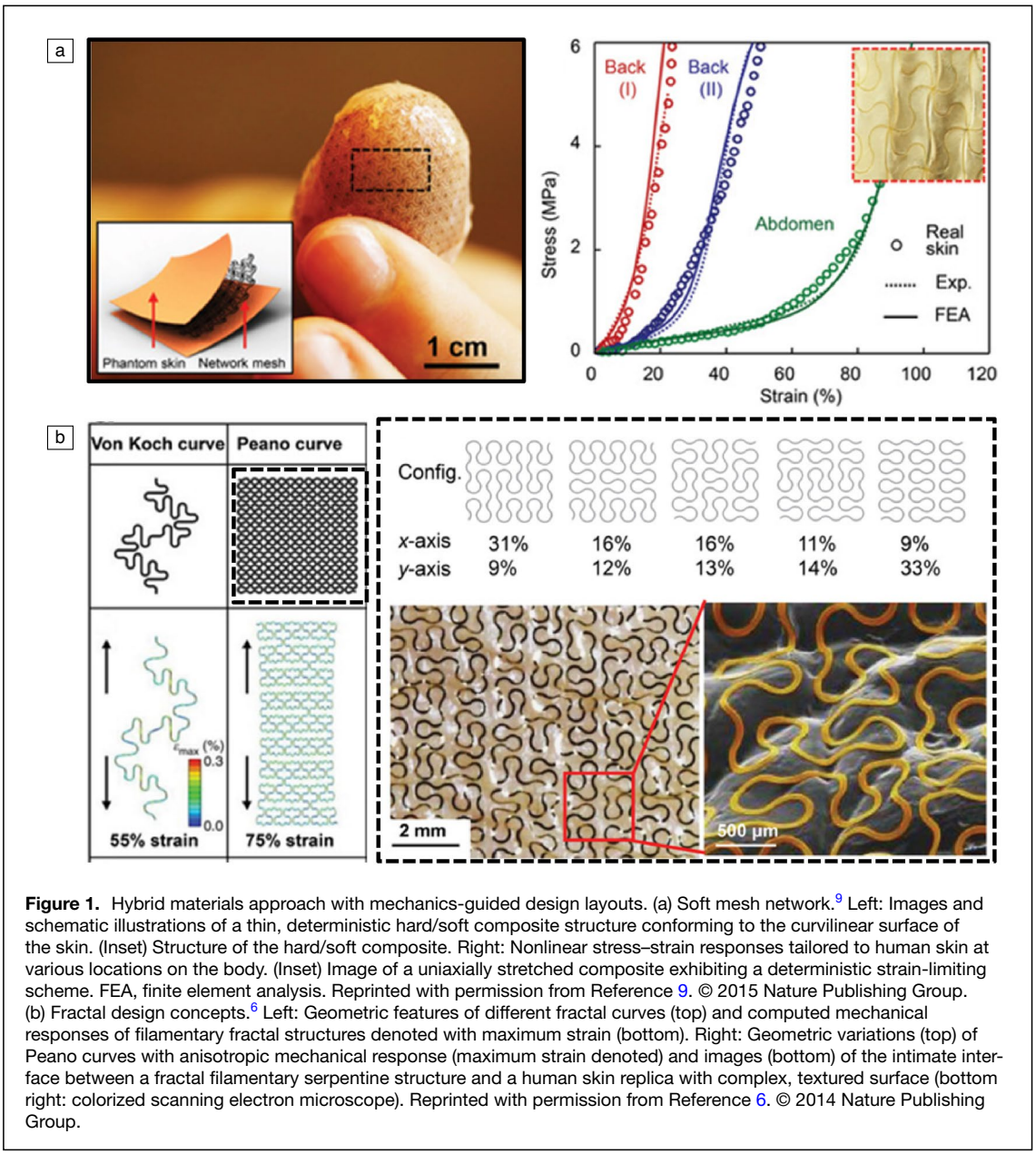

Figure 1. Hybrid materials approach with mechanics-guided design layouts. (a) Soft mesh network.[9] Left: Images and schematic illustrations of a thin, deterministic hard/soft composite structure conforming to the curvilinear surface of the skin. (Inset) Structure of the hard/soft composite. Right: Nonlinear stress–strain responses tailored to human skin at various locations on the body. (Inset) Image of a uniaxially stretched composite exhibiting a deterministic strain-limiting scheme. FEA, finite element analysis. Reprinted with permission from Reference 9. © 2015 Nature Publishing Group. (b) Fractal design concepts.[6] Left: Geometric features of different fractal curves (top) and computed mechanical responses of filamentary fractal structures denoted with maximum strain (bottom). Right: Geometric variations (top) of Peano curves with anisotropic mechanical response (maximum strain denoted) and images (bottom) of the intimate interface between a fractal filamentary serpentine structure and a human skin replica with complex, textured surface (bottom right: colorized scanning electron microscope). Reprinted with permission from Reference 6. © 2014 Nature Publishing Group.

tomography. All of these considerations, from circuit-level functionality to soft, skin-like mechanics, to compatibility with imaging techniques and radio-frequency power transfer and data communication, can be realized in these hybrid materials systems. A pair of wirelessly time-synchronized devices of this type can support the full range of functions supported by clinical standard technologies. Advanced versions support cost structures that are compatible with deployment even in resource-limited regions of importance in global health.[10]

In addition to sensors, a wide range of actuator technologies can be incorporated into the epidermal electronics platform. One example involves delivery of electrical, thermal, and/or mechanical stimulation impulses to the skin for haptic sensations across selected anatomical regions, including the entire body for enhanced experiences in VR/AR (i.e., virtual/augmented reality) applications and for patient feedback and rehabilitation, to complement video and audio inputs. The skin, as the largest organ of the body (areal coverage of ~2 m^2 of an adult human), provides the main source of physical perception of the world through mechano- and thermoreceptors at densities of up to 500 per cm^3. As with epidermal electronics for sensing, technologies to simulate realistic haptic cues must conform to the skin in a comfortable manner, but with the additional requirement for individually addressing these receptors over large areas, and with spatiotemporal control of multimodal forms of vibrational and temperature stimuli.[11] The level of complexity and multifunctionality in operation demands high-performance materials, integrated in hybrid layouts that are physically skin compatible. Figure 2b

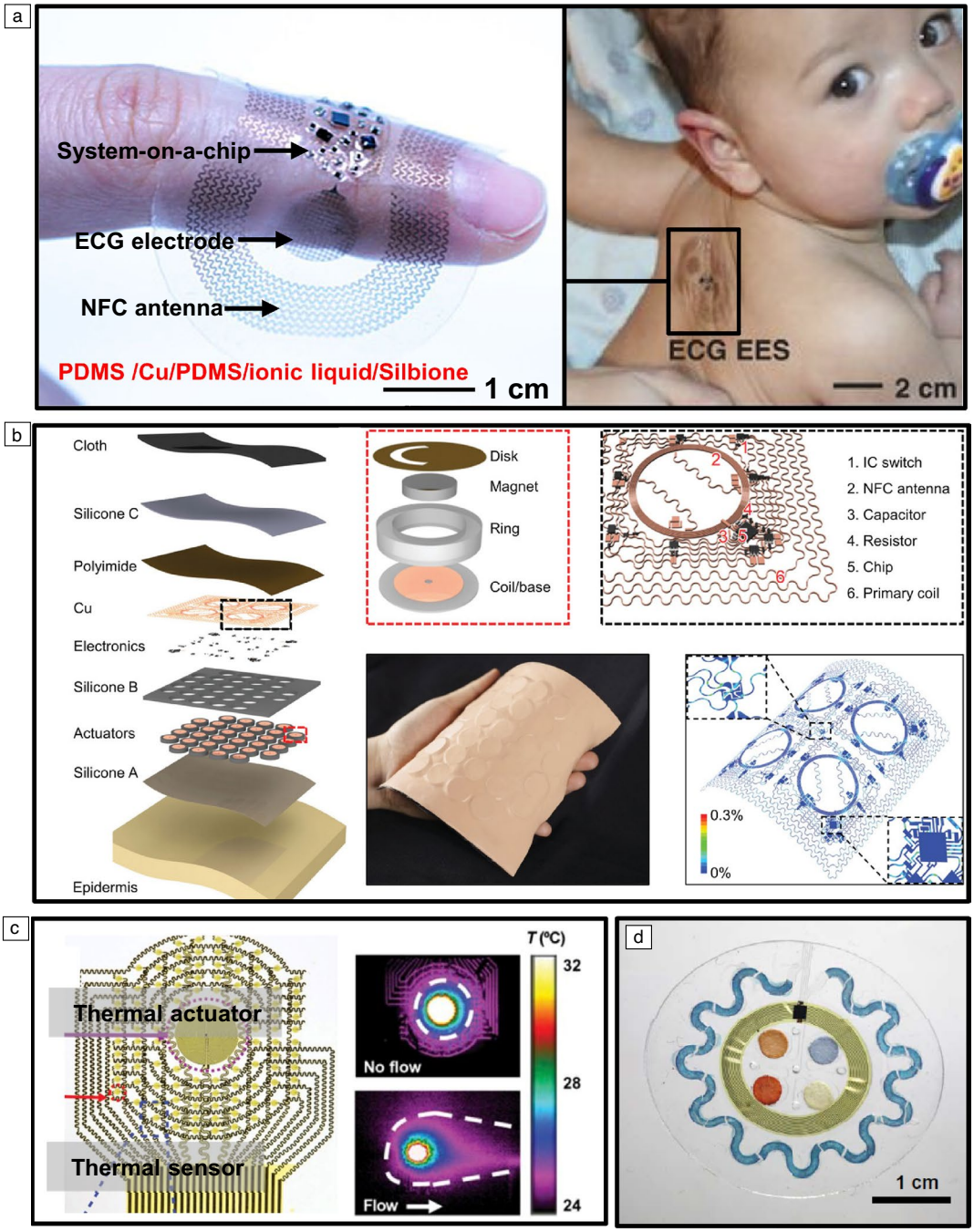

Figure 2. Epidermal electronic and microfluidic systems. (a) Left: Image of an epidermal electronic system (EES) that integrates capabilities in recording electrocardiograms, capturing wireless power, and supporting wireless communications into an ultrathin, soft skin-like platform with a hybrid materials approach. (Source: https://techxplore.com/news/2019-02-wires-cuddles-sensors-babies-nicu.html) Right: Image of the device worn on a neonate during clinical trials, illustrating an ability to follow natural deformations of the skin.[10] ECG, electrocardiogram. Reprinted with permission from Reference 10. © 2019 AAAS. (b) Schematic illustrations and images of a wirelessly powered and controlled epidermal haptic interface. Left: Exploded view illustration of the hybrid construction. Dashed boxes: Design of the magnetic actuator, control circuit, and computational interface, illustrating effective mechanical flexibility.[12] IC, integrated circuit. NFC, near-field communication. Reprinted with permission from Reference 12. © 2019 Nature Publishing Group. (c) Image of a noninvasive, skin-like flow monitoring device (left), and infrared images of the temperature distribution with and without flow associated with a near-surface blood vessel (right).[7] Reprinted with permission from Reference 7. © 2018 AAAS. (d) Image of a soft epidermal microfluidic device for capture, storage, and biochemical analysis of microliter volumes of sweat.[16] Reprinted with permission from Reference 16. © 2016 AAAS.

shows a wireless "epidermal" VR haptic interface constructed based on the hybrid materials approach, as a first example of this concept. The functional layer consists of filamentary serpentine Cu traces (thickness: 18 μm; width: 50–200 μm) configured using design strategies adapted from those demonstrated in the EES example above, mounted on a thin layer of polyimide (thickness: 12.5 μm), along with circuit components, passive elements, and control interfaces to a collection of haptic actuators built using soft PDMS materials, coils and rare earth magnets. A layer of silicone encapsulates and supports the system. A breathable, stretchable fabric coated with a thin film of silicone on top provides additional protection, while a thin elastomeric bottom layer serves as a gentle adhesive interface to the skin. Here, each actuator, tuned to resonate at frequencies, 100–300 Hz, that match the peak sensitivity in the skin, consists of a magnet-in-cavity construct, where power and control of Lorenz force-driven vibrations pass through a RF loop antenna. An array of 32 actuators (spatial density ~1 cm^2) can be individually addressed through a wireless NFC protocol with system-on-a-chip and integrated circuits. An island-bridge design with serpentine interconnects enables effective device flexibility for conformal attachment to various places of the body.[12] Advanced versions include multimodal stimulation (e.g., multimodal vibration, electrical stimulation, temperature modulation), as well as integrated sensors for feedback control.[13]

As with these actuators, other unusual components can be incorporated into epidermal electronics systems for monitoring modalities that lie beyond those of current clinical technologies. For example, a skin-like, noninvasive device, shown in Figure 2c, provides a low-cost, continuous monitoring capability for assessing flow of biofluids through micro- or macrovessels near the surface of the skin, applicable not only in hospital settings but also in the home.[7] This system incorporates a thin-film metallic (Cr/Au, thickness: 10/50 nm) actuator as a controlled source thermal power (dia.: 5 mm) surrounded by an array of resistive temperature sensors (50 sets; dia.: 0.5 mm) with serpentine interconnects (two layers of Ti/Cu/Ti/Au 20/600/20//25 nm; interlayer dielectric: PI), in an overall platform with exceptionally low thermal mass. Encapsulation layers of polyimide (thickness: 3 μm) and a soft elastomeric substrate (silicone, thickness: 100 μm) provide soft mechanical properties and physical robustness. The ultrathin (~100 μm), soft (E ~ 70 kPa), and lightweight (<10 mg/cm^2) skin-like physical properties minimize thermal impedances at the biointerface, for fast thermal mapping at milli-Kelvin precision[7,14] with negligible influence on natural thermal fluctuations of the skin. With a small input thermal power from the actuator, the sensors capture subtle spatiotemporal dynamics of heat flows through the skin. When placed above a near-surface macrovessel (artery/vein) or shunt (implanted tube to redirect cerebrospinal fluid), the resulting data can determine volumetric flow rates with the use of computation models. This system is particularly useful in functional assessment of shunts used to treat hydrocephalus patients, where failure rates reach 100% over a 5–10-yr. period and lead to nonspecific symptoms. Detection of malfunctioning shunts currently requires CT scans, x-rays, and sometimes surgeries that expose patients to various risks. The device featured in Figure 2c provides a low-cost, continuous monitoring capability for shunt flow assessment.[7]

Other forms of biofluid analysis follow from integration of microfluidic technologies for capture, analysis, and storage of pristine volumes of eccrine sweat that emerge from the surface of the skin.[15] This modification expands the epidermal platform from biophysical operation to biochemical assays. Figure 2d shows a structure of PDMS with a network of microchannels, microvalves, and reservoirs, in a hybrid configuration that allows conformal, watertight seals to the surface of the skin for sweat collection.[16] An appropriate formulation of PDMS with low modulus (~1 MPa) and skin compatibility can be manipulated using the techniques of soft lithography to define microfluidic structures as the basis for the devices (dia.: 3 cm; thickness: ~700 μm). Enriched silanol groups (Si–OH) on the surface of the PDMS enable fast and strong bonding with itself and to a layer of SiO_2 the bottom of an optional electronics module. A medical-grade acrylic adhesive film with thin geometry (25 μm) and low modulus (~17 kPa) ensures reliable bonding to the skin (~5.7 N). This collection of hybrid materials not only allows watertight sealing and integrity of the microfluidic system but also enables comfortable interfaces to the body, without leakage. The optical transparency of PDMS allows for use of chromogenic reagents/materials for optical readout. Serpentine channels and reservoirs allow visualization of the filling front, as sweat naturally pumps from the eccrine glands through inlets in the skin-facing side of the device. Imaging allows for determination of the local sweat rate and total sweat loss, of relevance to management of hydration in medical and sports contexts. Colorimetric or fluorometric chemistries enable quantitative assessment of biomarker concentrations (e.g., Figure 2d: chloride, glucose, pH, lactate) through digital analysis of images captured with a smartphone. Chromogenic reagents for the detection of chloride, glucose, pH, and lactate consist of mixtures of glucose oxidase, horseradish peroxidase, trehalose, and potassium iodide in sodium citrate buffer solution, mercury(II) thiocyanate, a universal indicator, and lactate dehydrogenase, respectively. Clinical tests on pediatric patients demonstrate utility for diagnosis of cystic fibrosis within and outside of clinical settings.[17] Deployments on athletes during competition and training provide real-time, personalized recommendations for fluid–electrolyte intake.[18]

Tissue-like implantable and neural interface

For implantable systems, related classes of hybrid materials technologies can be used in bioelectronics that operate via continuous coupling to soft internal organs. Conventional implantable devices, such as cardiac pacemakers/defibrillators, cochlear implants, and deep brain neurostimulators, interface with the soft tissues through simple metal electrodes,

hardwired to rigid housings that insulate the electronics. Complications in addressing schemes and noise considerations place limits on the ability to increase the numbers and densities of such passive electrodes. Hybrid approaches such as those described previously circumvent these limitations by allowing co-location of active, flexible electronics with the electrodes.[19,20] A persistent challenge is in materials for biofluid barriers—where the encapsulating structures must be sufficiently thin (i.e., a few micrometers or less) to allow mechanical flexibility, but sufficiently impermeable to isolate active materials from surrounding biofluids over time scales that could extend to the lifetime of the patient. Polymers and related organic films cannot satisfy such requirements, due to their various levels of permeability to water. Here, the hybrid approach, combining organic and inorganic materials, is an essential aspect of achieving chronic and high-performance operations.

Examples are in conformal sheets that wrap around the tissues of the heart and the brain. **Figure 3**a shows an example that delivers multiparametric physiological mapping and stimulation for cardiac electrotherapy with spatiotemporal control—functions not achievable with conventional lead-based cardiac implants.[8] Materials for these systems include thin, patterned layers of Ti/Au (5/300 nm) as interconnects and electrodes, PI (1.2 μm) as insulating interlayers, nanotextured platinum–iridium (Pt–Ir) alloys and poly(3,4-ethylenedioxythiophene)poly(styrene sulfonate) (PEDOT:PSS) for low impedance electrical interfaces, silicone elastomers ($E \sim 60$ kPa) as the mechanical supports, and filamentary serpentine traces of Au (width: 15 μm, thickness: 70 nm) as resistive temperature sensors. Enabling features of the platform are high-performance inorganic components (ranging from electrical, thermal, and optical stimulators, to sensors for pH, temperature, and mechanical strain) interconnected with serpentine traces for engineered stretchability, in combination with an elastomeric substrate designed to match the shape of the epicardial surface.[21] This collection of hybrid materials includes indium gallium nitride (InGaN) and aluminum indium gallium phosphide (AlInGaP) in microscale inorganic light-emitting diodes (μ-ILEDs, 300×300 μm^2, thickness: 3 μm) for optical mapping and dye excitation, silicon (Si) nanomembranes (thickness: 320 nm) for strain gauges, Au electrodes (1×1 mm^2) for electrical sensing/stimulation, iridium oxide (IrO_x)/Au pads (1×1 mm^2) for pH sensors, and Cr/Au serpentine resistors for temperature sensors/heaters (5/200 and 5/40 nm; dielectric: PI). Further advances employ fractal designs as previously discussed to realize large-area electrodes with uncompromised stretchability. Chronic stability requires high-performance barrier materials. Figure 3b demonstrates an active, kiloscale, neural interface for micro-electrocorticography (μ-ECoG) that employs a thin, transferred layer (900 nm) of SiO_2 thermally grown on a device-grade silicon wafer as a defect-free barrier layer with ultralow water vapor transmission rate (~10^{-6}–10^{-8} g m^{-2} d^{-1} at 25°C, 100% RH). Arrays of silicon nanomembrane-based n-channel complementary metal–oxide–semiconductor transistors (gate dielectric: Al_2O_3, metal interconnects: Cr/Au 5/200 nm, interlayer dielectric: PI) support active buffer and multiplexing transistors, enabling kiloscale electrodes over small areas (~9×9.24 mm^2). The resulting thin-film construct (~29 μm) is mechanically flexible to allow mounting on the curved surface of the dura (bending radius <2 mm) with chronically stable function *in vivo* for over a year.[22]

Other architectures involve injectable, compliant filamentary probes that integrate cellular-scale optoelectronics, microelectrodes, and thermal sensors for operation at locations in the deep brain.[23] Microscale inorganic InGaN μ-ILEDs (6.45-μm thick, 50×50 μm^2) exploit high-quality epitaxial material grown on sapphire and subsequently released by laser transfer, lithographically processed to establish contacts and patterned for individually addressable multicolored arrays. Transfer-printed to thin, microneedle-shaped polyester supports (thickness: <7 μm), these μ-ILED arrays can integrate with other similarly fabricated flexible devices, such as platinum (Pt) microelectrodes (20×20 μm^2, thickness: 100 nm), silicon-based photodetectors (thickness: 1.25 μm, 200×200 μm^2), and serpentine traces of Pt as resistive temperature sensors (thickness: 20 nm, width: 20 μm), in multilayer designs to deliver precision multimodal stimulation and sensing capabilities at desired anatomical sites. These compliant probes insert into the tissues via a rigid epoxy microneedle shuttle that releases upon dissolution of a bioresorbable interfacial adhesive. Figure 3c shows an example that combines an array of InGaN μ-ILEDs (active components of optofluidic probes, 100×100 μm^2, 6.54-μm thick) for optogenetic stimulation with PDMS microfluidic channels (10×10 μm^2, thickness: 50 μm) for programmed pharmacology.[24] Thin stainless steel microneedles (thickness: 50 μm), serving as insertion shuttles, bond to the soft, mechanically compliant optofluidic probes using water-soluble, purified silk (7 wt%), to enable release after implantation. A wireless control module enables versatile neuroscience experimental options in awake, freely behaving animals. A thermally expandable polymer (2:1 mixture of PDMS and expandable microspheres) acts as a mechanical transducer to initiate pumping activated using serpentine traces of Cr/Au (5/185 nm) as resistive heating elements. Properly encapsulated devices support chronic operation in freely moving animals without altering their natural behavior, due to the minimal invasiveness and mechanical compliance of these systems.[23–26] For example, cyclic olefin polymer-based reservoirs, chosen for low water vapor permeability (0.023 g·mm/m^2·day), with inner walls coated with parylene (thickness: 6 μm) and outlets sealed using thin copper membranes (thickness: 3 μm) provide necessary features in liquid retention and chemical resistance.

Building on the island-bridge design principle introduced earlier, stretchable, fully implantable, wireless system-level electronics are also possible, as shown in Figure 3d.[27] Here, the RF power harvesting antenna is engineered into serpentine constructs to enable stretchability; the thin-film Ti/Au

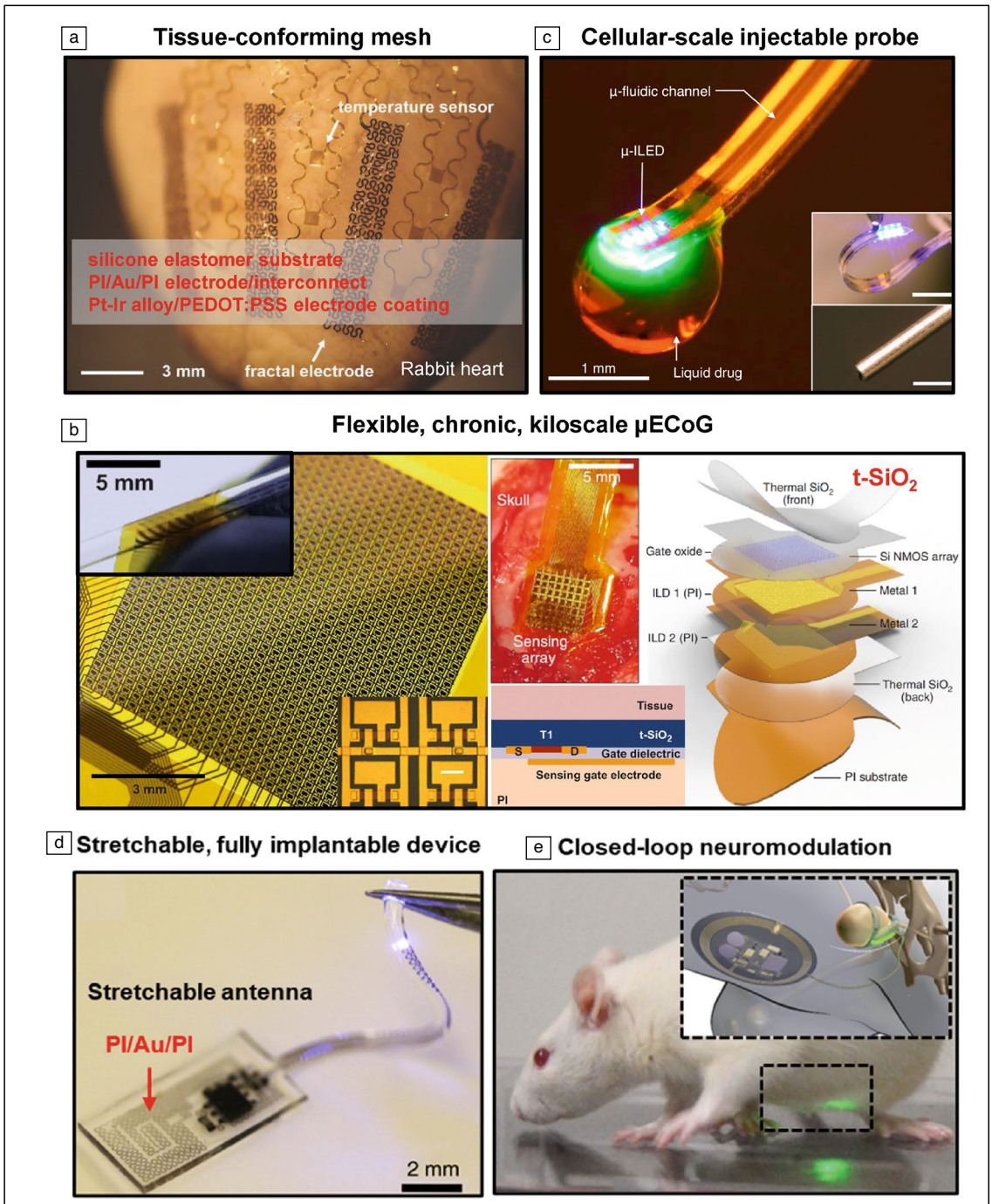

Figure 3. Tissue-like implantable neural interface technologies. (a) Image of a hybrid soft mesh covering the full epicardial surface of a Langendorff-perfused rabbit heart for multiparametric cardiac electrotherapy.[8] Reprinted with permission from Reference 8. © 2015 Wiley. (b) Left: Image of a 1008 channel flexible, chronic, active micro-electrocorticography (μ-ECoG) array. (Bottom inset) Image of each electrode connected to two silicon nanomembrane transistors. Scale bar = 100 μm. (Top inset) Image of a device bent around a cylindrical tube (dia.: 2.5 mm). Middle: A 64-ch μ-ECoG array implanted over rat auditory cortex (top), and schematic illustration of the operation (bottom). Right: Exploded view illustration highlighting thermally grown silicon dioxide as encapsulation for chronic operation.[22] ILD, interlayer dielectric. NMOS, n-channel metal oxide semiconductor. Reprinted with permission from Reference 22. © 2020 AAAS. (c) Image of an optofluidic neural probe for simultaneous drug delivery and photo-stimulation with cellular-scale micro-inorganic light-emitting diodes (μ-ILEDs). (Insets) Images of such a probe and a conventional metal cannula. Scale bars = 1 mm.[24] Reprinted with permission from Reference 24. © 2015 Elsevier. (d) Image of a soft, stretchable optogenetic device.[27] Reprinted with permission from Reference 27. © 2015 Nature Publishing Group. (e) Image of a rat with a fully implanted optoelectronic stimulation and sensing module. (Inset) Schematic illustration showing the stimulator and sensor on the bladder, connected to a subcutaneously implanted wireless power and control module.[28] Reprinted with permission from Reference 28. © 2019 Nature Publishing Group.

electrical traces (thickness: 3 μm) for both the antenna and the interconnects are encapsulated with PI (width: 40 μm, thickness: 3 μm). The resulting freestanding inorganic system embeds in a low-modulus silicone elastomer (~0.5 MPa, thickness: 100 μm), such that the final hybrid device exhibits low effective modulus (~1.7 MPa) to accommodate anatomical shapes and natural animal motions. This system enables reliable operation for neurocircuit activation of both peripheral and spinal pain circuits in freely moving mice.

This implantable platform can be configured as an autonomous bioelectronic form of medicine, where the wireless system-on-a-chip supports power, communication, and computation in a hybrid materials construct that extends multimodal stimulation/sensing nodes deployed on various tissues. Advanced versions can enable closed-loop feedback-controlled forms of therapy based on real-time diagnostic monitoring. Figure 3e shows a soft, fully implanted device that autonomously regulates bladder dysfunction in freely moving mice, where the system monitors bladder volume with a resistive strain sensor formed using a silicone polymer doped with carbon black (thickness: 15 μm).[28] Algorithms provide real-time analyses of pathological behavior, for purposes of initiating autonomous optogenetic neuromodulation on the bladder sensory afferents to normalize bladder function. The system, encapsulated using a low-modulus silicone formulation (thickness: 40 μm, $E \sim 60$ kPa) shows stable operation *in vivo* after one month of implantation. Another bioelectronic medicine platform combines diagnostic modalities of electroencephalograms (EEGs), electromyograms (EMGs), and body temperature, with therapeutic modalities of optical stimulation and drug delivery units, all autonomously controlled by onboard electronics.[29] Platinum black and polydopamine modified Au electrodes (thickness: 100 nm, diameter: 0.9 mm) enable low interface impedances for EEG recording. The fully implantable device captures neurorecordings with quality similar to gold-standard wired systems, with on-device artificial intelligence for real-time analytics. A bilayer coating of parylene and PDMS (thickness of each layer: 30 μm) provides mechanical and electrical protection. Demonstrations show these combined capabilities in chronic operation (six weeks) in freely moving mice for sleep–wake regulation studies and closed-loop epileptic seizure treatment via EEG-triggered pharmacological suppression.

Transient electronics

An interesting alternative to chronic bioelectronic implantable systems is in electronics designed to disappear without a trace over a lifetime aligned with application requirements. This "transient" technology provides a basis for temporary biomedical implants, with stable operation throughout a designated biological process (e.g., 4–6 weeks for wound healing) followed by natural bioresorption (or bioabsorption; [e.g., through metabolic actions]) to circumvent the associated costs, risks, and potential for complications in surgical extraction procedures. The first example of a high-performance, fully bioresorbable electronic device exploits Si NMs (thickness: 300 nm) as the semiconductor, with Mg (thickness: 200–800 nm) as the conductor, MgO (thickness: 150–600 nm) and SiO_2 (thickness: 100 nm) as the dielectrics and silk fibroin (thickness: 50–100 μm) as the substrate and encapsulant, as reported in 2012.[30] The key enabling observation is that Si NMs with thicknesses in the range of a few tens of hundreds of nanometers naturally dissolve in biofluids over relevant time scales (days, weeks, and months), as the foundation for a hybrid approach in a silicon-based form of transient bioelectronics. Subsequent studies establish a wide range of inorganic bioresorbable electronic materials, along with the fundamental materials science associated with their dissolution in biofluids.[31,32] The transience processes include passive and active types, where the former involves dissolution that initiates upon deployment (i.e., usually through hydrolysis upon contact with biofluid), and the latter relies on an initiating stimulus.[33] The passive mode is often sufficient for most biomedical applications.

In well-designed passive transient systems, the initial stages of bioresorption affect only the encapsulation structure, thereby ensuring stable operation of the underlying active devices. Breach of the encapsulation and initial dissolution of the active materials represents the end of the functional lifetime. Subsequent degradation leads to mechanical disintegration, complete material bioresorption and eventual excretion from the body. For example, SiO_2, the inorganic insulating material frequently used in commercial electronics as gate dielectrics, passivation coatings and water barriers, dissolves in water by hydrolysis reactions similar to those that apply to Si NMs ($SiO_2 + 2H_2O \rightarrow Si(OH)_4$). The rates depend on the deposition/growth method through its density and stoichiometry (phosphate-buffered saline [PBS], pH 7.4, 37°C: ~10 nm/day, e-beam; 0.01 nm/day, thermally grown, t-SiO_2).[34] Organic polymeric alternatives (e.g., silk fibroin) suffer from swelling and comparatively high rates of water permeation (Table I). Sufficiently thin films of t-SiO_2 (10 nm) as encapsulation layers support stable monitoring of intracranial pressure in rats for 25 days. Complete bioresorption occurs in less than a year based on studies of dissolution kinetics.[35] **Figure 4**a summarizes the dissolution rates of representative inorganic electronic materials under physiological conditions (PBS, pH 7.4, 37°C).[31] Silicon dissolves in aqueous media at near neutral pH conditions through hydrolysis ($Si + 4H_2O \rightarrow Si(OH)_4 + 2H_2$), at a rate of ~5 nm/day, implying that a ~100-nm-thick Si NM, typical in many forms of electronics, dissolves in ~20 days. Dissolution studies indicate a linear relationship between film thickness and time, as expected for mechanisms of surface erosion reactions. The dissolution rate increases with pH, consistent with the alkaline wet-etching chemistry for silicon. The temperature dependence of this rate also follows Arrhenius scaling. Monocrystalline silicon and other semiconductors (e.g., polycrystalline Si, amorphous Si, Ge, and Si-Ge alloy, ZnO), dielectrics (SiO_2, Si_3N_4), and conductors (Mg, Zn, W, Fe, Mo) form the inorganic materials library with

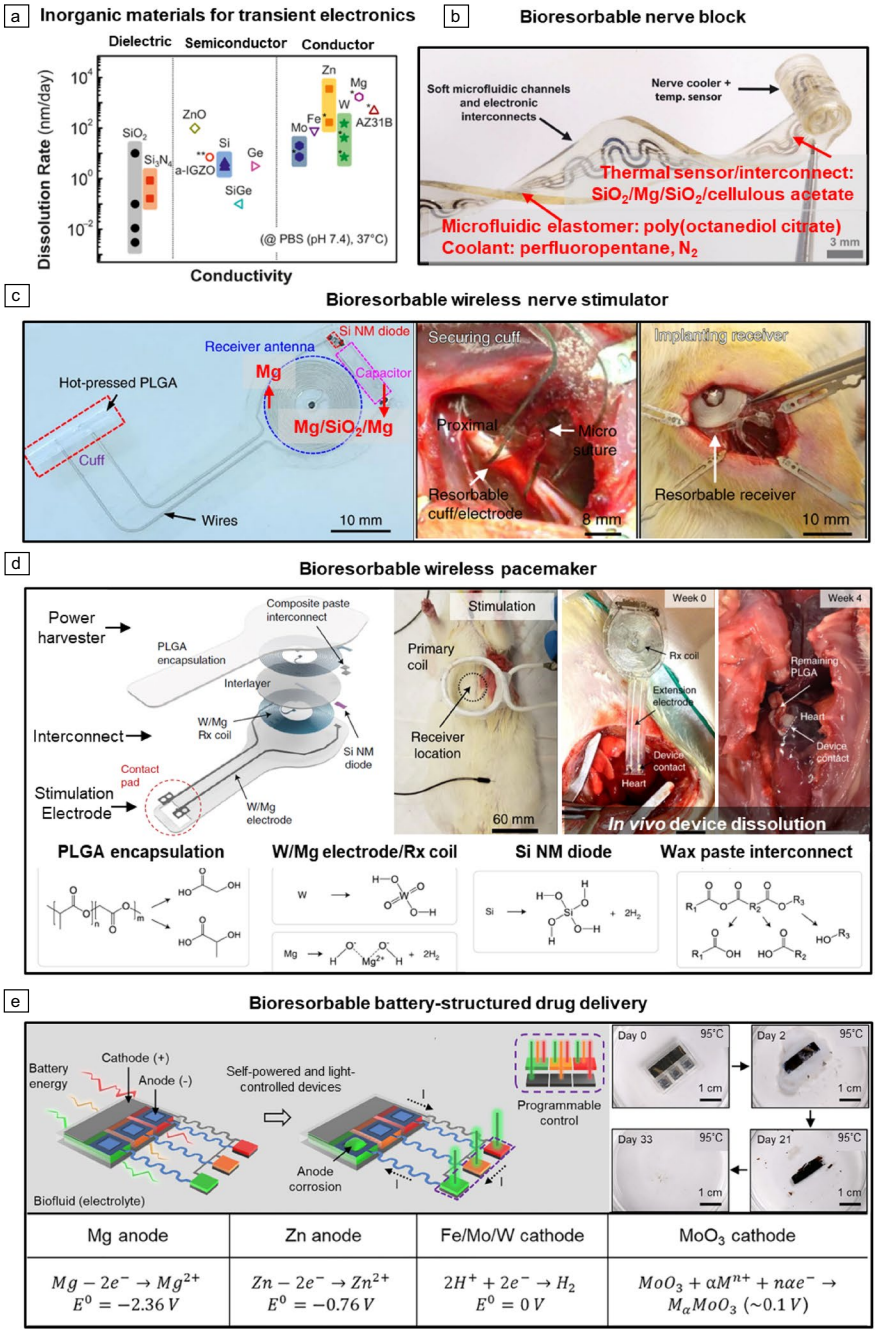

Figure 4. Transient electronic systems. (a) Representative bioresorbable inorganic electronic materials and their dissolution rates.[31] (b) Image of a soft, bioresorbable nerve cooler with elastomeric interconnects and a terminal cuff structure.[39] Reprinted with permission from Reference 39. © 2022 AAAS. (c) Left: Image of a bioresorbable, wireless electrical stimulator for neuroregenerative medicine. Middle: Image of a nerve cuff secured to the sciatic nerve of a rat. Right: Image of a radio-frequency harvester subcutaneously implanted.[40] Reprinted with permission from Reference 40. © 2018 Nature Publishing Group. (d) Schematic illustration of a fully implantable and bioresorbable cardiac pacemaker with dissolution routes of the constituent materials. (Insets) Images of a device implanted in a rat partially bioresorbed after a therapeutic period.[41] Reprinted with permission from Reference 41. © 2022 AAAS. (e) Top: Schematic diagram of light-controlled opening of drug reservoirs by electrochemical erosion of a metal gate, as the anode of a battery system (left). Image of *in vitro* dissolution of the battery unit (right). Bottom: Electrochemical reactions and standard potentials of bioresorbable anodes and cathodes.[42] NM, nanomembrane. Reprinted with permission from Reference 42. © 2023 National Academy of Sciences.

high-performance, wide-ranging electronic properties that can undergo passive transience.[31] Studies indicate that these materials and their hydrolysis products are biocompatible, as evaluated by histopathology, elemental biodistribution, hematology, and immunohistochemical stained high-resolution cross-sectional images.[31]

Examples of bioresorbable electronics as temporary implants range from actively addressed Si NM electrodes with multiplexing capabilities for spatiotemporal mapping of electrical activity from the cerebral cortex,[36] bioresorbable silicon sensors for intracranial pressure and temperature monitoring,[37] to bioresorbable photonic devices that monitor cerebral temperature, oxygenation, and neural activity.[38] A direction of particular interest is in temporary postoperative bioelectric therapy (wound healing), with stimulation and sensing capabilities that address medical needs (e.g., alternative pain management, improved neurodegenerative treatment and cardiac pacing) during a period of surgical recovery, and naturally disappear with a lifetime aligned to the healing process to avoid extraction surgeries. In postoperative pain management, where addictive drugs can be problematic, peripheral nerve cooling presents a promising approach to block pain signals due to its rapid reversibility and location precision. Figure 4b shows a hybrid microfluidic and electronic system that provides on-demand local analgesia via cooling of a peripheral nerve followed by subsequent device dissolution and bioresorption.[39] A bioresorbable elastomer (poly(octanediol citrate), thickness: 240 μm) defines microfluidic channels that mix a bioinert liquid coolant (perfluoropentane) and nitrogen sealed at the nerve cuff to realize reversible cooling through liquid-to-gas phase transition (sustained nerve cooling to ~3°C). A bioresorbable thin-film resistive temperature sensor composed of SiO_2/Mg/SiO_2 (thickness: 100/300/100 nm, width: 25 μm, length: 72 mm, substrate: 50-μm-thick cellulose acetate) monitors the temperature of the nerve in real time, enabling closed-loop control. Multiweek *in vivo* trials demonstrate its ability to rapidly and precisely cool peripheral nerves to provide local, on-demand analgesia in rat models for neuropathic pain, and *in vitro* test shows full device dissolution and bioabsorption in 50 days (PBS at 75°C, pH 7.4).

Fully wireless technologies are also possible, as illustrated by the programmable nerve stimulator in Figure 4c.[40] The device, encapsulated with poly(lactic-*co*-glycolic acid) (65:35 lactide:glycolide; thickness: 30 μm), consists of a receiving antenna (Mg, thickness: 50 μm), a rectifier (Mg/SiO_2/Mg capacitor, thickness: 50 μm/600 nm/50 μm, Si NM diode: 320-nm-thick Si NM and 300-nm-thick Mg electrical contacts), and a nerve cuff stimulator (Mg or Mo electrodes, thickness: 50-μm Mg or 10-μm Mo, width: 340 μm). Inductive coupling to an external transmission antenna (at ~5 MHz, maximum separation distance ~80 mm) delivers cathodic, monophasic electrical impulses (duration: 200 μs; threshold voltage: 100–300 mV) to the interfaced region of the nerve. The addition of wax encapsulation (thickness: 300 μm) for the inorganic active materials (Mg/Mo, SiO_2, Si NM) extends the lifetime and supports programmed stimulation for up to six days *in vivo*, with full bioresorption of all active materials after 25 days (PBS at 37°C, pH 7.4). This system can enhance peripheral neurodegeneration and functional recovery of damaged nerves, as demonstrated in rodent models.[40] A related device technology can be used as a temporary cardiac pacemaker, with similar layouts and hybrid materials described above (Figure 4d).[41] Combined use with a skin-interfaced module that senses cardiac rhythms and communicates to the implanted pacemaker through magnetic inductive coupling allows for closed-loop, autonomous electrotherapy.

Bioresorbable batteries offer alternatives to wireless power transfer strategies, as in the example of the actively programmable drug delivery device in Figure 4e. Here, the encapsulated drug and the surrounding biofluid act as electrolytes for the battery, while the anodes (Mg, Mg coated with spin-on-glass, or Zn in millimeter scale; thickness: 10–100 μm), which form gate valves for the underlying drug reservoir, connect to the cathode (Fe, Mo, W, or MoO_3 in millimeter-scale geometries; thickness: 5–50 μm) through a phototransistor. External illumination activates the phototransistor, thereby short-circuiting the anode and cathode, causing accelerated corrosion of the anode and thus opening of the reservoir gate. Wavelength-division multiplexing enables programmable release of multiple drugs.[42] Another representative example involves eco/bioresorbable magnesium-iodine batteries (Mg thickness: 200 μm) with ionic liquid (a mixture of choline chloride and urea) and aqueous media in a dual-electrolyte design.[43] This collection of hybrid materials significantly improves the voltage (~1.8 V), areal capacity (~10 $mA \cdot h \cdot cm^{-2}$), areal energy (~17.7 $mWh \cdot cm^{-2}$), areal power (~0.7 $mW \cdot cm^{-2}$), volumetric energy (~93.0 $mWh \cdot cm^{-3}$), and volumetric power densities (~3.8 $mW \cdot cm^{-3}$) and enables power supply for wireless wearable systems, microcontrollers, temperature sensors, resistive heating elements, and cardiac pacemakers.

Three-dimensional electronics

The hybrid materials approaches discussed thus far focus on devices that interact with the surfaces of organs (e.g., skin, heart, brain, bladder, etc.) or at localized positions in their depths, with noninvasive/minimally invasive operation due to favorable mechanical and geometrical properties. Biology, by contrast, is inherently 3D, with designs that commonly involve open 3D architectures of both hard and soft materials, hierarchical across a broad range of length scales, multifunctional and reconfigurable. Examples include open scaffolds of neural circuits, vasculature networks, and cytoskeletal meshes. Designing 3D, mesoscale open networks capable of integration with biology through these volumetric spaces represents an exciting future for bioelectronics. A goal, then, in rendering planar device technologies (i.e., electronics, optoelectronics, microfluidics) into well-defined 3D network architectures requires capabilities beyond those supported by current 3D printing techniques (e.g., direct ink writing, stereolithography),[44] to allow integration of high-quality semiconductor

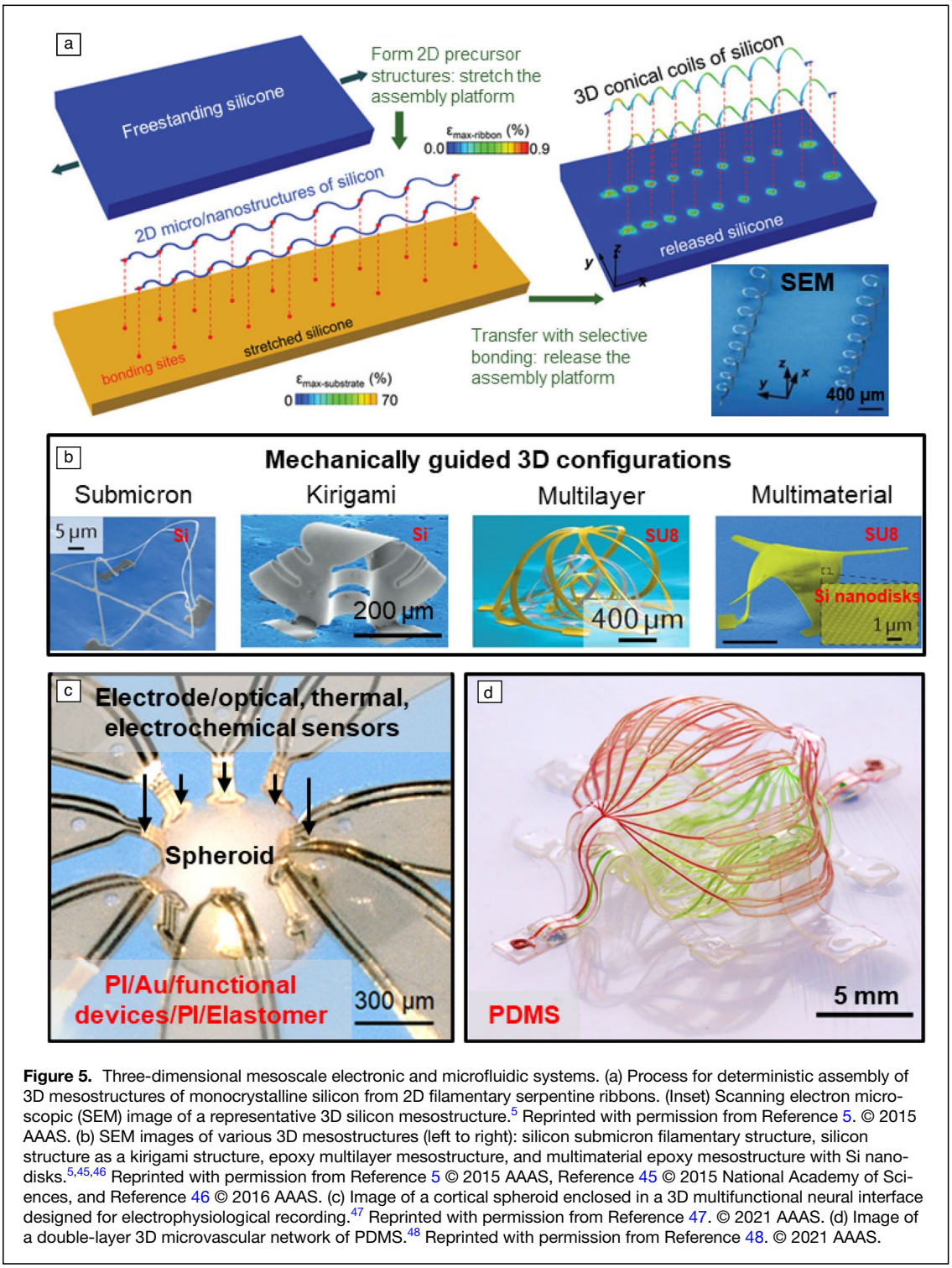

Figure 5. Three-dimensional mesoscale electronic and microfluidic systems. (a) Process for deterministic assembly of 3D mesostructures of monocrystalline silicon from 2D filamentary serpentine ribbons. (Inset) Scanning electron microscopic (SEM) image of a representative 3D silicon mesostructure.[5] Reprinted with permission from Reference 5. © 2015 AAAS. (b) SEM images of various 3D mesostructures (left to right): silicon submicron filamentary structure, silicon structure as a kirigami structure, epoxy multilayer mesostructure, and multimaterial epoxy mesostructure with Si nanodisks.[5,45,46] Reprinted with permission from Reference 5 © 2015 AAAS, Reference 45 © 2015 National Academy of Sciences, and Reference 46 © 2016 AAAS. (c) Image of a cortical spheroid enclosed in a 3D multifunctional neural interface designed for electrophysiological recording.[47] Reprinted with permission from Reference 47. © 2021 AAAS. (d) Image of a double-layer 3D microvascular network of PDMS.[48] Reprinted with permission from Reference 48. © 2021 AAAS.

devices, ideally in schemes that adopt the principles of hybrid materials integration.

One successful strategy exploits mechanics-guided assembly mechanisms for geometrically transforming planar, 2D microsystems into 3D architectures via programmed buckling driven by relaxation of a prestrained elastomeric substrate.[5] The process begins with conventional and slightly modified methods in thin-film deposition and semiconductor device processing to yield 2D filamentary structures similar to those described previously. Liftoff from a supporting substrate allows transfer printing to a prestrained elastomer substrate, with patterned surface chemistry to ensure strong bonding only at lithographically defined locations. Release of the substrate imposes in-plane stresses on the mesh structure at these bonding sites, thereby

causing a controlled buckling process that creates a corresponding 3D structure through coordinated translation and rotational motions of the unbonded regions, programmable by the geometry of the precursor, the configuration of bonding sites, and the nature and magnitude of the prestrain. **Figure 5a** shows the controlled buckling process and a representative resulting structure formed from 2D serpentine silicon ribbons (thickness: 2 μm, width: 50 μm) with spatial gradients in their arc radii.[5] Deterministic 3D geometries can be captured by finite element analysis across extensive length scales (i.e., nanometers to centimeters). The process is compatible with nearly all classes of thin-film materials and device technologies. Figure 5b shows representative 3D silicon and epoxy mesostructures and hybrid nanomembrane systems (silicone-epoxy), as foundations for advanced functional 3D devices.[5,45,46]

Three-dimensional tissue constructs (i.e., spheroids, organoids, and assembloids) derived from human stem cells are increasingly important in studies of patient-specific responses to drugs and other therapies. Conventional 2D device platforms fail to provide useful interfaces due to the geometry mismatch. Three-dimensional structures that wrap around such 3D tissues can deliver multimodal neuromodulation, sensing, and manipulation capabilities, with broad opportunities in neuroscience research. Figure 5c features a 3D multifunctional framework designed to study a cortical spheroid.[47] Computationally guided by FEA, the 3D device envelops the spheroid through a collection of concave-shaped wings, each made of thin-film PI (4 μm) and functionalized with active components, specifically including platinum black-coated Au microelectrodes (dia.: 50 μm) for both recording and electrical stimulation, InGaN μ-ILEDs for optical stimulation, Au thermal actuators and temperature gauges with filamentary serpentine structures (thickness: 200 nm, width: 3 μm) for closed-feedback loop control, and electrochemical sensors (platinum black, Au, and Ag/AgCl as working, counter, and reference electrodes, respectively; size: 250 μm × 300 μm) for measuring the local oxygen concentration. Studies of cortical spheroids conducted using such platforms include spreading coordinated bursting events on a single spheroid, and the cascading processes across a pair of spheroids (assembloids) during neuroregeneration.[47] Similar mechanics-guided assembly approaches can also realize 3D PDMS microfluidic constructs with geometries (e.g., double-layered with branching channels) and feature sizes (e.g., 5–10 μm, mammalian capillary) that resemble biological vascular networks (Figure 5d). The ability to distribute fluids and to interrogate various biological processes across volumetric spaces creates many exciting opportunities to study 3D cell cultures, engineered tissues, and artificial organs.[48]

Conclusions

As illustrated in this article, hybrid materials approaches form a powerful basis for electronic technologies designed for intimate functional integration with soft living tissues. The capabilities support a broad range of unique and enabling options in sensing and therapeutic action, including closed-loop operation. These strategies combine the best attributes of both organic and inorganic materials in composite structures of thin films, micro-/nanoscale architectures, 3D frameworks, and supporting matrices, to offer versatile choices in engineering design. Although this article narrowly focuses on our own work, many other groups have made critically important contributions, as part of a growing, worldwide collection of materials research efforts in this area. Opportunities for further research include development of materials that enable (1) advanced capabilities in biochemical sensing, to complement well-established and expanding modes for biophysical sensing; (2) electrical, pharmaceutical, thermal, and other forms of pain management, accelerated healing, and cancer treatment; (3) multimodal, closed-loop feedback control over therapeutic operation based on outputs from the sensors, or on intrinsically responsive, multifunctional constructs; (4) mechanical actuation as artificial muscles for rehabilitation, haptic interfaces, and modes of user feedback; (5) energy harvesting, using schemes based on biofuel cells, piezoelectric/triboelectric materials, photovoltaics, and others; (6) advanced batteries and supercapacitors for power storage; and (7) chronically stable operation in tissue-integrated implants. Efforts in manufacturing science will also be important in translating these technologies from academic prototypes to devices that can be cost-effectively deployed at scale. Activities in these and other directions, from fundamental studies in materials science to applied efforts in device engineering, represent compelling, diverse prospects for research, of additional interest due to the relevance of successful outcomes to grand challenges in global health.

Data availability

Not applicable.

Conflict of interest

J.A.R. is a co-founder of startup companies that are pursuing commercialization of certain technologies described in this article.

References

1. K.W. Cho, S.H. Sunwoo, Y.J. Hong, J.H. Koo, J.H. Kim, S. Baik, T. Hyeon, D.H. Kim, *Chem. Rev.* **122**, 5068 (2022)
2. Q.S. Yang, Z.Y. Hu, J.A. Rogers, *Acc. Mater. Res.* **2**, 1010 (2021)
3. E.M. Song, J.H. Li, S.M. Won, W.B. Bai, J.A. Rogers, *Nat. Mater.* **19**, 590 (2020)
4. D.T. Simon, E.O. Gabrielsson, K. Tybrandt, M. Berggren, *Chem. Rev.* **116**, 13009 (2016)
5. S. Xu, Z. Yan, K.I. Jang, W. Huang, H.R. Fu, J. Kim, Z. Wei, M. Flavin, J. McCracken, R. Wang, A. Badea, Y. Liu, D.Q. Xiao, G.Y. Zhou, J. Lee, H.U. Chung, H.Y. Cheng, W. Ren, A. Banks, X.L. Li, U. Paik, R.G. Nuzzo, Y.G. Huang, Y.H. Zhang, J.A. Rogers, *Science* **347**, 154 (2015)
6. J.A. Fan, W.H. Yeo, Y.W. Su, Y. Hattori, W. Lee, S.Y. Jung, Y.H. Zhang, Z.J. Liu, H.Y. Cheng, L. Falgout, M. Bajema, T. Coleman, D. Gregoire, R.J. Larsen, Y.G. Huang, J.A. Rogers, *Nat. Commun.* **5**, 3266 (2014)
7. S.R. Krishnan, T.R. Ray, A.B. Ayer, Y.J. Ma, P. Gutruf, K. Lee, J.Y. Lee, C. Wei, X. Feng, B. Ng, Z.A. Abecassis, N. Murthy, I. Stankiewicz, J. Freudman, J. Stillman, N. Kim, G. Young, C. Goudeseune, J. Ciraldo, M. Tate, Y.G. Huang, M. Potts, J.A. Rogers, *Sci. Transl. Med.* **10**, eaat8437 (2018)
8. L.Z. Xu, S.R. Gutbrod, Y.J. Ma, A. Petrossians, Y.H. Liu, R.C. Webb, J.A. Fan, Z.J. Yang, R.X. Xu, J.J. Whalen, J.D. Weiland, Y.G. Huang, I.R. Efimov, J.A. Rogers, *Adv. Mater.* **27**, 1731 (2015)

9. K.I. Jang, H.U. Chung, S. Xu, C.H. Lee, H.W. Luan, J. Jeong, H.Y. Cheng, G.T. Kim, S.Y. Han, J.W. Lee, J. Kim, M. Cho, F.X. Miao, Y.Y. Yang, H.N. Jung, M. Flavin, H. Liu, G.W. Kong, K.J. Yu, S.I. Rhee, J. Chung, B. Kim, J.W. Kwak, M.H. Yun, J.Y. Kim, Y.M. Song, U. Paik, Y.H. Zhang, Y. Huang, J.A. Rogers, *Nat. Commun.* **6**, 6566 (2015)
10. H.U. Chung, B.H. Kim, J.Y. Lee, J. Lee, Z.Q. Xie, E.M. Ibler, K. Lee, A. Banks, J.Y. Jeong, J. Kim, C. Ogle, D. Grande, Y. Yu, H. Jang, P. Assem, D. Ryu, J.W. Kwak, M. Namkoong, J.B. Park, Y. Lee, D.H. Kim, A. Ryu, J. Jeong, K. You, B.W. Ji, Z.J. Liu, Q.Z. Huo, X. Feng, Y.J. Deng, Y.S. Xu, K.I. Jang, J. Kim, Y.H. Zhang, R. Ghaffari, C.M. Rand, M. Schau, A. Hamvas, D.E. Weese-Mayer, Y.G. Huang, S.M. Lee, C.H. Lee, N.R. Shanbhag, A.S. Paller, S. Xu, J.A. Rogers, *Science* **363**, 947 (2019)
11. H.D. Bai, S. Li, R.F. Shepherd, *Adv. Funct. Mater.* **31**(39), 2009364 (2021)
12. X.G. Yu, Z.Q. Xie, Y. Yu, J. Lee, A. Vazquez-Guardado, H.W. Luan, J. Ruben, X. Ning, A. Akhtar, D.F. Li, B.W. Ji, Y.M. Liu, R.J. Sun, J.Y. Cao, Q.Z. Huo, Y.S. Zhong, C. Lee, S. Kim, P. Gutruf, C.X. Zhang, Y.G. Xue, Q.L. Guo, A. Chempakasseril, P.L. Tian, W. Lu, J. Jeong, Y. Yu, J. Cornman, C. Tan, B. Kirn, K. Lee, X. Feng, Y.G. Huang, J.A. Rogers, *Nature* **575**(7783), 473 (2019)
13. Y.H. Jung, J.Y. Yoo, A. Vazquez-Guardado, J.H. Kim, J.T. Kim, H.W. Luan, M. Park, J. Lim, H.S. Shin, C.J. Su, R. Schloen, J. Trueb, R. Avila, J.K. Chang, D.S. Yang, Y. Park, H. Ryu, H.J. Yoon, G. Lee, H. Jeong, J.U. Kim, A. Akhtar, J. Cornman, T.I. Kim, Y.G. Huang, J.A. Rogers, *Nat. Electron.* **5**, 621 (2022)
14. R.C. Webb, A.P. Bonifas, A. Behnaz, Y.H. Zhang, K.J. Yu, H.Y. Cheng, M.X. Shi, Z.G. Bian, Z.J. Liu, Y.S. Kim, W.H. Yeo, J.S. Park, J.Z. Song, Y.H. Li, Y.G. Huang, A.M. Gorbach, J.A. Rogers, *Nat. Mater.* **12**, 1078 (2013)
15. D.S. Yang, R. Ghaffari, J.A. Rogers, *Science* **379**, 760 (2023)
16. A. Koh, D. Kang, Y. Xue, S. Lee, R.M. Pielak, J. Kim, T. Hwang, S. Min, A. Banks, P. Bastien, M.C. Manco, L. Wang, K.R. Ammann, K.-I. Jang, P. Won, S. Han, R. Ghaffari, U. Paik, M.J. Slepian, G. Balooch, Y.G. Huang, J.A. Rogers, *Sci. Transl. Med.* **8**(366), 366ra165 (2016). https://doi.org/10.1126/scitranslmed.aaf2593
17. T.R. Ray, M. Ivanovic, P.M. Curtis, D. Franklin, K. Guventurk, W.J. Jeang, J. Chafetz, H. Gaertner, G. Young, S. Rebollo, J.B. Model, S.P. Lee, J. Ciraldo, J.T. Reeder, A. Hourlier-Fargette, A.J. Bandodkar, J. Choi, A.J. Aranyosi, R. Ghaffari, S.A. McColley, S. Haymond, J.A. Rogers, *Sci. Transl. Med.* **13**(587), eabd8109 (2021). https://doi.org/10.1126/scitranslmed.abd8109
18. L.B. Baker, J.B. Model, K.A. Barnes, M.L. Anderson, S.P. Lee, K.A. Lee, S.D. Brown, A.J. Reimel, T.J. Roberts, R.P. Nuccio, J.L. Bonsignore, C.T. Ungaro, J.M. Carter, W.H. Li, M.S. Seib, J.T. Reeder, A.J. Aranyosi, J.A. Rogers, R. Ghaffari, *Sci. Adv.* **6**(50), eabe3929 (2020). https://doi.org/10.1126/sciadv.abe3929
19. T.M. Fu, G.S. Hong, R.D. Viveros, T. Zhou, C.M. Lieber, *Proc. Natl. Acad. Sci. U.S.A.* **114**, E10046 (2017)
20. I.R. Minev, P. Musienko, A. Hirsch, Q. Barraud, N. Wenger, E.M. Moraud, J. Gandar, M. Capogrosso, T. Milekovic, L. Asboth, R.F. Torres, N. Vachicouras, Q. Liu, N. Pavlova, S. Duis, A. Larmagnac, J. Voros, S. Micera, Z. Suo, G. Courtine, S.P. Lacour, *Science* **347**, 159 (2015)
21. L.Z. Xu, S.R. Gutbrod, A.P. Bonifas, Y.W. Su, M.S. Sulkin, N.S. Lu, H.-J. Chung, K.-I. Jang, Z.J. Liu, M. Ying, C. Lu, R.C. Webb, J.-S. Kim, J.I. Laughner, H.Y. Cheng, Y.H. Liu, A. Ameen, J.-W. Jeong, G.-T. Kim, Y.G. Huang, I.R. Efimov, J.A. Rogers, *Nat. Commun.* **5**, 3329 (2014)
22. C.-H. Chiang, S.M. Won, A.L. Orsborn, K.J. Yu, M. Trumpis, B. Bent, C. Wang, Y.G. Xue, S. Min, V. Woods, C.X. Yu, B.H. Kim, S.B. Kim, R. Huq, J.H. Li, K.J. Seo, F. Vitale, A. Richardson, H. Fang, Y.G. Huang, K. Shepard, B. Pesaran, J.A. Rogers, J. Viventi, *Sci. Transl. Med.* **12**(538), eaay4682 (2020)
23. T.I. Kim, J.G. McCall, Y.H. Jung, X. Huang, E.R. Siuda, Y.H. Li, J.Z. Song, Y.M. Song, H.A. Pao, R.H. Kim, C.F. Lu, S.D. Lee, I.S. Song, G. Shin, R. Al-Hasani, S. Kim, M.P. Tan, Y.G. Huang, F.G. Omenetto, J.A. Rogers, M.R. Bruchas, *Science* **340**, 211 (2013)
24. J.W. Jeong, J.G. McCall, G. Shin, Y.H. Zhang, R. Al-Hasani, M. Kim, S. Li, J.Y. Sim, K.I. Jang, Y. Shi, D.Y. Hong, Y.H. Liu, G.P. Schmitz, L. Xia, Z.B. He, P. Gamble, W.Z. Ray, Y.G. Huang, M.R. Bruchas, J.A. Rogers, *Cell* **162**, 662 (2015)
25. Y.Y. Yang, M.Z. Wu, A. Vazquez-Guardado, A.J. Wegener, J.G. Grajales-Reyes, Y.J. Deng, T.Y. Wang, R. Avila, J.A. Moreno, S. Minkowicz, V. Dumrongprechachan, J. Lee, S.Y. Zhang, A.A. Legaria, Y.H. Ma, S. Mehta, D. Franklin, L. Hartmann, W.B. Bai, M.D. Han, H.B. Zhao, W. Lu, Y. Yu, X. Sheng, A. Banks, X.G. Yu, Z.R. Donaldson, R.W. Gereau, C.H. Good, Z.Q. Xie, Y.G. Huang, Y. Kozorovitskiy, J.A. Rogers, *Nat. Neurosci.* **24**, 1035 (2021)
26. Y.X. Wu, M.Z. Wu, A. Vázquez-Guardado, J. Kim, X. Zhang, R. Avila, J.-T. Kim, Y.J. Deng, Y. Yu, S. Melzer, Y. Bai, H. Yoon, L.Z. Meng, Y. Zhang, H.X. Guo, L. Hong, E.E. Kanatzidis, C.R. Haney, E.A. Waters, A.R. Banks, Z.Y. Hu, F. Lie, L.P. Chamorro, B.L. Sabatini, Y.G. Huang, Y. Kozorovitskiy, J.A. Rogers, *Nat. Commun.* **13**(1), 5571 (2022)
27. S.I. Park, D.S. Brenner, G. Shin, C.D. Morgan, B.A. Copits, H.U. Chung, M.Y. Pullen, K.N. Noh, S. Davidson, S.J. Oh, J. Yoon, K.-I. Jang, V.K. Samineni, M. Norman, J.G. Grajales-Reyes, S.K. Vogt, S.S. Sundaram, K.M. Wilson, J.S. Ha, R.X. Xu, T.S. Pan, T.-I. Kim, Y.G. Huang, M.C. Montana, J.P. Golden, M.R. Bruchas, R.W. Gereau IV, J.A. Rogers, *Nat. Biotechnol.* **33**, 1280 (2015)
28. A.D. Mickle, S.M. Won, K.N. Noh, J. Yoon, K.W. Meacham, Y.G. Xue, L.A. McIlvried, B.A. Copits, V.K. Samineni, K.E. Crawford, D.H. Kim, P. Srivastava, B.H. Kim, S. Min, Y. Shiuan, Y. Yun, M.A. Payne, J.P. Zhang, H. Jang, Y.H. Li, H.H. Lai, Y.G. Huang, S.I. Park, R.W. Gereau, J.A. Rogers, *Nature* **565**, 361 (2019)
29. W. Ouyang, W. Lu, Y. Zhang, Y. Liu, J.U. Kim, H. Shen, Y. Wu, H. Luan, K. Kilner, S.P. Lee, Y. Lu, Y. Yang, J. Wang, Y. Yu, A.J. Wegener, J.A. Moreno, Z. Xie, Y. Wu, S.M. Won, K. Kwon, C. Wu, W. Bai, H. Guo, T.L. Liu, H. Bai, G. Monti, J. Zhu, S.R. Madhvapathy, J. Trueb, M. Stanslaski, E.M. Higbee-Dempsey, I. Stepien, N. Ghoreishi-Haack, C.R. Haney, T.I. Kim, Y. Huang, R. Ghaffari, A.R. Banks, T.C. Jhou, C.H. Good, J.A. Rogers, *Nat. Biomed. Eng.* (2023). https://doi.org/10.1038/s41551-023-01029-x
30. S.W. Hwang, H. Tao, D.H. Kim, H.Y. Cheng, J.K. Song, E. Rill, M.A. Brenckle, B. Panilaitis, S.M. Won, Y.S. Kim, Y.M. Song, K.J. Yu, A. Ameen, R. Li, Y.W. Su, M.M. Yang, D.L. Kaplan, M.R. Zakin, M.J. Slepian, Y.G. Huang, F.G. Omenetto, J.A. Rogers, *Science* **337**, 1640 (2012)
31. Y. Choi, J. Koo, J.A. Rogers, *MRS Bull.* **45**(2), 103 (2020)
32. Q.S. Yang, Z.Y. Hu, M.-H. Seo, Y.M. Xu, Y. Yan, Y.-H. Hsu, J. Berkovich, K. Lee, T.-L. Liu, S. McDonald, H.L. Nie, H. Oh, M.Z. Wu, J.-T. Kim, S.A. Miller, Y. Jia, S. Butun, W.B. Bai, H.X. Guo, J. Choi, A. Banks, W.Z. Ray, Y. Kozorovitskiy, M.L. Becker, M.A. Pet, M.R. MacEwan, J.-K. Chang, H.L. Wang, Y.G. Huang, J.A. Rogers, *Nat. Commun.* **13**, 6518 (2022). https://doi.org/10.1038/s41467-022-34173-0
33. G. Lee, Y.S. Choi, H.J. Yoon, J.A. Rogers, *Matter* **3**, 1031 (2020)
34. S.K. Kang, S.W. Hwang, H.Y. Cheng, S. Yu, B.H. Kim, J.H. Kim, Y.G. Huang, J.A. Rogers, *Adv. Funct. Mater.* **24**, 4427 (2014)
35. J.H. Shin, Y. Yan, W.B. Bai, Y.G. Xue, P. Gamble, L.M. Tian, I. Kandela, C.R. Haney, W. Spees, Y. Lee, M. Choi, J. Ko, H. Ryu, J.K. Chang, M. Pezhouh, S.K. Kang, S.M. Won, K.J. Yu, J.N. Zhao, Y.K. Lee, M.R. MacEwan, S.K. Song, Y.G. Huang, W.Z. Ray, J.A. Rogers, *Nat. Biomed. Eng.* **3**, 37 (2019)
36. K.J. Yu, D. Kuzum, S.W. Hwang, B.H. Kim, H. Juul, N.H. Kim, S.M. Won, K. Chiang, M. Trumpis, A.G. Richardson, H.Y. Cheng, H. Fang, M. Thompson, H. Bink, D. Talos, K.J. Seo, H.N. Lee, S.K. Kang, J.H. Kim, J.Y. Lee, Y.G. Huang, F.E. Jensen, M.A. Dichter, T.H. Lucas, J. Viventi, B. Litt, J.A. Rogers, *Nat. Mater.* **15**, 782 (2016)
37. S.K. Kang, R.K.J. Murphy, S.W. Hwang, S.M. Lee, D.V. Harburg, N.A. Krueger, J.H. Shin, P. Gamble, H.Y. Cheng, S. Yu, Z.J. Liu, J.G. McCall, M. Stephen, H.Z. Ying, J. Kim, G. Park, R.C. Webb, C.H. Lee, S.J. Chung, D.S. Wie, A.D. Gujar, B. Vemulapalli, A.H. Kim, K.M. Lee, J.J. Cheng, Y.G. Huang, S.H. Lee, P.V. Braun, W.Z. Ray, J.A. Rogers, *Nature* **530**, 71 (2016)
38. W.B. Bai, J. Shin, R.X. Fu, I. Kandela, D. Lu, X.Y. Ni, Y. Park, Z.H. Liu, T. Hang, D. Wu, Y.H. Liu, C.R. Haney, I. Stepien, Q.S. Yang, J. Zhao, K.R. Nandoliya, H. Zhang, X. Sheng, L. Yin, K. MacRenaris, A. Brikha, F. Aird, M. Pezhouh, J. Hornick, W.D. Zhou, J.A. Rogers, *Nat. Biomed. Eng.* **3**, 644 (2019)
39. J.T. Reeder, Z.Q. Xie, Q.S. Yang, M.H. Seo, Y. Yan, Y.J. Deng, K.R. Jinkins, S.R. Krishnan, C. Liu, S. McKay, E. Patnaude, A. Johnson, Z.C. Zhao, M.J. Kim, Y.M. Xu, I. Huang, R. Avila, C. Felicelli, E. Ray, X. Guo, W.Z. Ray, Y.G. Huang, M.R. MacEwan, J.A. Rogers, *Science* **377**, 109 (2022)
40. J. Koo, M.R. MacEwan, S.K. Kang, S.M. Won, M. Stephen, P. Gamble, Z.Q. Xie, Y. Yan, Y.Y. Chen, J. Shin, N. Birenbaum, S.J. Chung, S.B. Kim, J. Khalifeh, D.V. Harburg, K. Bean, M. Paskett, J. Kim, Z.S. Zohny, S.M. Lee, R.Y. Zhang, K.J. Luo, B.W. Ji, A. Banks, H.M. Lee, Y.G. Huang, W.Z. Ray, J.A. Rogers, *Nat. Med.* **24**, 1830 (2018)
41. Y.S. Choi, R.T. Yin, A. Pfenniger, J. Koo, R. Avila, K.B. Lee, S.W. Chen, G. Lee, G. Li, Y. Qiao, A. Murillo-Berlioz, A. Kiss, S.L. Han, S.M. Lee, C.H. Li, Z.Q. Xie, Y.Y. Chen, A. Burrell, B. Geist, H. Jeong, J. Kim, H.J. Yoon, A. Banks, S.K. Kang, Z.J. Zhang, C.R. Haney, A.V. Sahakian, D. Johnson, T. Efimova, Y.G. Huang, G.D. Trachiotis, B.P. Knight, R.K. Arora, I.R. Efimov, J.A. Rogers, *Nat. Biotechnol.* **39**, 1228 (2021)
42. Y. Zhang, F. Liu, Y. Zhang, J. Wang, D. D'Andrea, J.B. Walters, S. Li, H.J. Yoon, M. Wu, S. Li, Z. Hu, T. Wang, J. Choi, K. Bailey, E. Dempsey, K. Zhao, A. Lantsova, Y. Bouricha, I. Huang, H. Guo, X. Ni, Y. Wu, G. Lee, F. Jiang, Y. Huang, C.K. Franz, J.A. Rogers, *Proc. Natl. Acad. Sci. U.S.A.* **120**(11), e2217734120 (2023)
43. I. Huang, Y.M. Zhang, H.M. Arafa, S.P. Li, A. Vazquez-Guardado, W. Ouyang, F. Liu, S. Madhvapathy, J.W. Song, A. Tzavelis, J. Trueb, Y. Choi, W.J. Jeang, V. Forsberg, E. Higbee-Dempsey, N. Ghoreishi-Haack, I. Stepien, K. Bailey, S.L. Han, Z.J. Zhang, C. Good, Y.G. Huang, A.J. Bandodkar, J.A. Rogers, *Energy Environ. Sci.* **15**, 4095 (2022)
44. J.A. Rogers, *MRS Bull.* **44**(3), 195 (2019)
45. Y.H. Zhang, Z. Yan, K.W. Nan, D.Q. Xiao, Y.H. Liu, H.W. Luan, H.R. Fu, X.Z. Wang, Q.L. Yang, J.C. Wang, W. Ren, H.Z. Si, F. Liu, L.H. Yang, H.J. Li, J.T. Wang, X.L. Guo, H.Y. Luo, L. Wang, Y.G. Huang, J.A. Rogers, *Proc. Natl. Acad. Sci. U.S.A.* **112**, 11757 (2015)
46. Z. Yan, F. Zhang, F. Liu, M.D. Han, D.P. Ou, Y.H. Liu, Q. Lin, X.L. Guo, H.R. Fu, Z.Q. Xie, M.Y. Gao, Y.M. Huang, J. Kim, Y.T. Qiu, K.W. Nan, J. Kim, P. Gutruf, H.Y. Luo, A. Zhao, K.-C. Hwang, Y.G. Huang, Y.H. Zhang, J.A. Rogers, *Sci. Adv.* **2**(9), e1601014 (2016). https://doi.org/10.1126/sciadv.1601014
47. Y. Park, C.K. Franz, H. Ryu, H.W. Luan, K.Y. Cotton, J.U. Kim, T.S. Chung, S.W. Zhao, A. Vazquez-Guardado, D.S. Yang, K. Li, R. Avila, J.K. Phillips, M.J. Quezada, H. Jang, S.S. Kwak, S.M. Won, K. Kwon, H. Jeong, A.J. Bandodkar, M.D. Han, H.B. Zhao, G.R. Osher, H.L. Wang, K. Lee, Y.H. Zhang, Y.G. Huang, J.D. Finan, J.A. Rogers, *Sci. Adv.* **7**(12), eabf9153 (2021). https://doi.org/10.1126/sciadv.abf9153
48. H.W. Luan, Q.H. Zhang, T.-L. Liu, X.J. Wang, S.W. Zhao, H.L. Wang, S.L. Yao, Y.G. Xue, J.W. Kwak, W.B. Bai, Y.M. Xu, M.D. Han, K. Li, Z.W. Li, X.C. Ni, J.L. Ye, D.W. Choi, Q.S. Yang, J.-H. Kim, S. Li, S.L. Chen, C.S. Wu, D. Lu, J.-K. Chang, Z.Q. Xie, Y.G. Huang, J.A. Rogers, *Sci. Adv.* **7**(43), eabj3686 (2021). https://doi.org/10.1126/sciadv.abj3686
49. A. Kalra, A. Lowe, A.M. Al-Jumaily, *J. Mater. Sci. Eng.* **5**(4), 100254 (2016)
50. S. Ramadan, N. Paul, H.E. Naguib, *Biomed. Mater.* **12**, 025013 (2017)

51. Y. Ling, W.B. Pang, J.X. Liu, M. Page, Y.D. Xu, G.G. Zhao, D. Stalla, J.W. Xie, Y.H. Zhang, Z. Yan, *Nat. Commun.* **13**, 524 (2022). https://doi.org/10.1038/s41467-022-28185-z
52. G.C. Engelmayr, M.Y. Cheng, C.J. Bettinger, J.T. Borenstein, R. Langer, L.E. Freed, *Nat. Mater.* **7**, 1003 (2008)
53. S. Budday, R. Nay, R. de Rooij, P. Steinmann, T. Wyrobek, T.C. Ovaert, E. Kuhl, *J. Mech. Behav. Biomed. Mater.* **46**, 318 (2015)
54. T.R. Ray, J. Choi, A.J. Bandodkar, S. Krishnan, P. Gutruf, L.M. Tian, R. Ghaffari, J.A. Rogers, *Chem. Rev.* **119**, 5461 (2019)
55. K.-I. Jang, K. Li, H.U. Chung, S. Xu, H.N. Jung, Y.Y. Yang, J.W. Kwak, H.H. Jung, J. Song, C. Yang, A. Wang, Z.J. Liu, J.Y. Lee, B.H. Kim, J.-H. Kim, J. Lee, Y. Yu, B.J. Kim, H. Jang, K.J. Yu, J. Kim, J.W. Lee, J.-W. Jeong, Y.M. Song, Y.G. Huang, Y.H. Zhang, J.A. Rogers, *Nat. Commun.* **8**, 15894 (2017). https://doi.org/10.1038/ncomms15894
56. D.H. Kim, J.H. Ahn, W.M. Choi, H.S. Kim, T.H. Kim, J.Z. Song, Y.G.Y. Huang, Z.J. Liu, C. Lu, J.A. Rogers, *Science* **320**, 507 (2008)
57. D.H. Kim, J.Z. Song, W.M. Choi, H.S. Kim, R.H. Kim, Z.J. Liu, Y.Y. Huang, K.C. Hwang, Y.W. Zhang, J.A. Rogers, *Proc. Natl. Acad. Sci. U.S.A.* **105**, 18675 (2008)

Hedan Bai is an assistant professor of robotic materials in the Department of Materials at ETH Zürich, Switzerland, since 2023. She received her BS degree from Cornell University with a double major in mechanical engineering, and operations research and information engineering in 2016. She obtained her MS and PhD (2021) degrees in mechanical engineering from Cornell University, where her thesis studied multimodal and self-healing soft optical sensors. In 2021, Bai joined the Querrey Simpson Institute for Bioelectronics at Northwestern University as a postdoctoral scholar and focused on soft robotic bioelectronics for minimally invasive surgery. Her research interests center on building physical intelligence into devices through soft materials and optics for advanced biomedical and robotic functions. Bai can be reached by email at hedan.bai@mat.ethz.ch.

Ziying Hu is a postdoctoral scholar in the Querrey Simpson Institute for Bioelectronics at Northwestern University. She received her BS degree in materials science and engineering from Wuhan University of Science and Technology, China, in 2011, MS degree in applied chemistry from Beihang University, China, in 2014, and her MS degree in materials science and engineering from the University of California, San Diego, in 2016. In 2020, she received her PhD degree in chemistry from Northwestern University. Her research interests include bioelectronics, manufacturing technologies, bio-/bioinspired materials, and soft matter. Hu can be reached by email at ziying.hu@northwestern.edu.

John A. Rogers is the Louis Simpson and Kimberly Querrey Professor of Materials Science and Engineering, Biomedical Engineering and Neurological Surgery, and the director of the Querrey Simpson Institute for Bioelectronics at Northwestern University. His awards include a MacArthur Fellowship in 2009, the Lemelson-MIT Prize in 2011, the Materials Research Society Medal in 2018, and the Benjamin Franklin Medal in 2019. He is a member of the National Academy of Engineering, the National Academy of Sciences, the National Academy of Medicine, and the American Academy of Arts & Sciences. Rogers can be reached by email at jrogers@northwestern.edu.